CX_3CR1^+ Cell – Mediated *Salmonella* Exclusion Protects the Intestinal Mucosa during the Initial Stage of Infection

Angela L. Man,*,[1] Nadezhda Gicheva,*,[1] Mari Regoli,[†] Gary Rowley,[‡] Giovanna De Cunto,[†] Nikolaus Wellner,[x] Elizabeth Bassity,* Massimo Gulisano,[{] Eugenio Bertelli,[†,2] and Claudio Nicoletti*,[{,2]

During *Salmonella* Typhimurium infection, intestinal CX_3CR1^+ cells can either extend transepithelial cellular processes to sample luminal bacteria or, very early after infection, migrate into the intestinal lumen to capture bacteria. However, until now, the biological relevance of the intraluminal migration of CX_3CR1^+ cells remained to be determined. We addressed this by using a combination of mouse strains differing in their ability to carry out CX_3CR1-mediated sampling and intraluminal migration. We observed that the number of *S.* Typhimurium traversing the epithelium did not differ between sampling-competent/migration-competent C57BL/6 and sampling-deficient/migration-competent BALB/c mice. In contrast, in sampling-deficient/migration-deficient $CX_3CR1^{2/2}$ mice the numbers of *S.* Typhimurium penetrating the epithelium were significantly higher. However, in these mice the number of invading *S.* Typhimurium was significantly reduced after the adoptive transfer of CX_3CR1^+ cells directly into the intestinal lumen, consistent with intraluminal CX_3CR1^+ cells preventing *S.* Typhimurium from infecting the host. This interpretation was also supported by a higher bacterial fecal load in $CX_3CR1^{+/gfp}$ compared with $CX_3CR1^{gfp/gfp}$ mice following oral infection. Furthermore, by using real-time in vivo imaging we observed that CX_3CR1^+ cells migrated into the lumen moving through paracellular channels within the epithelium. Also, we reported that the absence of CX_3CR1-mediated sampling did not affect Ab responses to a noninvasive *S.* Typhimurium strain that specifically targeted the CX_3CR1-mediated entry route. These data showed that the rapidly deployed CX_3CR1^+ cell – based mechanism of immune exclusion is a defense mechanism against pathogens that complements the mucous and secretory IgA Ab – mediated system in the protection of intestinal mucosal surface.

One of the main tasks of the epithelium overlying mucosal surfaces of the intestinal tract is to provide an effective barrier to microorganisms present in the intestinal lumen. First, this is achieved by the presence of tight junctions that allow the passage of water and ions but provide an effective mechanical barrier to macromolecules and microbes (1). Second, a combination of thick flowing mucus and secretory IgA (sIgA) bathing mucosal surfaces provides an efficient gel that sequestrates harmful microorganisms and prevents them from crossing the epithelial barrier in a process known as immune exclusion (2, 3). Furthermore, it has been recently shown that a few hours after infection the epithelium-intrinsic NAIP/NLRC4 inflammasone drove the expulsion of infected epithelial cells to restrict *Salmonella* Typhimurium replication in the mucosa (4). Ultimately, the aim of these protective mechanisms is to prevent pathogens from traversing/colonizing the intestinal mucosa. We have previously reported that intestinal challenge with *S.* Typhimurium induced, very shortly after infection, the migration into the intestinal lumen of *S.* Typhimurium – capturing cells expressing the high-affinity receptor CX_3CR1 for the chemokine fractalkine (CX_3CL1) into the intestinal lumen (5), a chemokine that although expressed by a variety of cells is produced at its highest level by the intestinal epithelial cells (IECs) of the ileum (6). The migration of CX_3CR1^+ cells following challenge with *S.* Typhimurium was restricted to the small intestine in a flagellin/MyD88-dependent manner and did not affect the integrity of the epithelial barrier (5). These observations prompted us to test the hypothesis that *Salmonella*-capturing CX_3CR1^+ cells migrate rapidly into the intestinal lumen to limit the number of pathogens crossing the epithelial barrier. Interestingly, in the occurrence of infection with *S.* Typhimurium, CX_3CR1^+ cells displayed a dual behavior. Indeed, these cells can also directly sample bacteria by using cellular extensions that protrude between epithelial cells and shuttle them across the epithelium to initiate immune responses (7, 8). Importantly, the presence of the fractalkine receptor CX_3CR1 appeared to be essential for both events (6, 9). However, although CX_3CR1-mediated sampling plays a role in the generation of immune responses (7), the biological relevance of the intraluminal migration of the

*Gut Health and Food Safety Programme, Institute of Food Research, Norwich NR4 7UA, United Kingdom; [†]Department of Molecular and Developmental Medicine, University of Siena, 53100 Siena, Italy; [‡]School of Biological Sciences, University of East Anglia, Norwich NR4 7TJ, United Kingdom; [x]Analytical Sciences Unit, Institute of Food Research, Norwich NR4 7UA, United Kingdom; and [{]Section of Human Anatomy, Department of Experimental and Clinical Medicine, University of Florence, 50134 Florence, Italy

[1]A.L.M. and N.G. contributed equally to this paper.

[2]E. Bertelli and C.N. contributed equally to this paper.

ORCIDs: 0000-0002-9681-4556 (E. Bertelli); 0000-0002-6242-4867 (C.N.).

This work was supported by the Biotechnology and Biological Sciences Research Council Institute Strategic Programme Grant BB/J004529/1 (The Gut Health and Food Safety Institute Strategic Programme) (to C.N.) and by intramural funds from the University of Siena (to E. Bertelli).

Address correspondence and reprint requests to Dr. Claudio Nicoletti at the current address: Department of Experimental and Clinical Medicine, Section of Human Anatomy, University of Florence, Florence, Italy. E-mail: claudio.nicoletti@unifi.it or claudio.nicoletti@ifr.ac.uk

Abbreviations used in this article: AFC, Ab-forming cell; IEC, intestinal epithelial cell; MLN, mesenteric lymph node; PP, Peyer's patch; sIgA, secretory IgA; TEM, transmission electron microscopy; wt, wild-type.

CX_3CR1^+ cells during the early stages of infection remained to be determined. We sought to address this issue by using a combination of mouse strains that differed in their ability to undergo CX_3CR1-mediated direct sampling and intraluminal migration during *S.* Typhimurium infection. Indeed, whereas wild-type (wt) C57BL/6 mice responded to *S.* Typhimurium with CX_3CR1-mediated sampling (8) and migration (5), wt BALB/c mice lacked the ability to sample luminal Ag via this route (sampling deficient) (10) but were migration competent (5). Furthermore, these two mouse strains were complemented with CX_3CR1-deficient mice that were both sampling and migration deficient (6, 9). We observed that the rapid *Salmonella*-induced intraluminal migration of CX_3CR1^+ cells reduced significantly the bacterial load in the intestinal tissue, thus contributing effectively to the immune exclusion provided by the mucous barrier and sIgA-based system.

Materials and Methods

Mice

Six- to eight-week-old female $CX_3CR1^{gfp/gfp}$, BALB/c, and C57BL/6 background mice (11) were used as CX_3CR1-deficient mice and bred with wt BALB/c or C57BL/6 mice to obtain heterozygote $CX_3CR1^{+/gfp}$ mice. $CX_3CR1^{2/2}$ (C57BL/6 background) mice were purchased from Taconic, and 6- to 8-wk-old wt BALB/c and C57BL/6 mice were purchase from Charles River Laboratories. Villin-Cre MyD88 ($MyD88^{\Delta IEC}$) (C57BL/6 background) mice were from the Welcome Trust Sanger Institute (Hinxton, U.K.) (12). CX_3CR1^6 and $CX_3CR1^{2/2}$ mice on the $RAG^{2/2}$ background (B6.129S7-*Rag1*^{tm1Mom}/J; The Jackson Laboratory) were obtained by an intercross between the knockout mice. Mice on the $RAG^{2/2}$ background were kept in a specific pathogen-free high-barrier environment. Overall, mice were kept under standardized conditions in groups of three to five per cage. Food and water were provided ad libitum. Experiments were conducted under the guidelines of the Scientific Procedure Animal Act (1986) of the U.K. or at the University of Siena under the "Guiding Principles for Research Involving Animals and Human Beings." Intestinal surgery was performed under terminal anesthesia induced and maintained throughout the procedure by inhalation of isoflurane.

Bacteria

The *S.* Typhimurium SL1344 Δ*invA*::kan mutant was constructed using the lambda Red recombination system as described previously (13). Briefly, using primers invARed forward (5′-TGAAAAGCTGTCTTAATTTAA-TATTAACAGGATACCTATA-3′) and invARed reverse (5′-ATATC-CAAATGTTGCATAGATCTTTTCCTTAATTAAGCCC-3′) the entire coding sequence of *invA* was replaced by a flippase recognition target-flanked Km cassette from template plasmid pKD4. Recombinants were selected for kanamycin resistance and verified by PCR. The mutation was subsequently transduced by P22 into a clean SL1344 parent background and into SL3261 (*Aro*^{2}) to construct the double mutation.

Bacterial challenge

Isolated loops were injected with 1×10^7 noninvasive/nonreplicating *InvA*^{2}*Aro*^{2} for intravital imaging experiments or invasive/nonreplicating *InvA*$^+$*AroA*^{2} *S.* Typhimurium for collecting intraluminal $CX_3CR1^{+/gfp}$ cells for phenotypic and quantitative analyses. Oral challenges were performed by gavages that were delivered 5 – 10 min after administration of a solution of $NaHCO_3$ (10% [w/v] per 200 μl). To monitor intraluminal migration of CX_3CR1^+ cell or bacterial load in the gut tissue within 5 h postinfection, mice received a single oral dose of 1×10^7 of either *InvA*$^+$*AroA*^{2}, *InvA*^{2}*AroA*^{2}, or *InvA*^{2}*AroA*$^+$ *S.* Typhimurium; to determine long-term (5 d postinfection) bacterial load, mice received a single dose of 1×10^7 *InvA*^{2}*Aro*$^+$ strain. To determine strain-specific susceptibility to *S.* Typhimurium infection, mice received a single dose of 1×10^8 wt *InvA*$^+$*AroA*$^+$ *S.* Typhimurium; finally, to investigate Ab responses to noninvasive *S.* Typhimurium, mice received three doses of 1×10^8 *InvA*^{2}*Aro*^{2} at 3-d intervals. To monitor intraluminal migration of CX_3CR1^+ cells and fecal bacterial load, mice received a single oral dose of 1×10^7 *InvA*$^+$*Aro*^{2} *S.* Typhimurium. To determine translocation of noninvasive *Inv*^{2} *S.* Typhimurium, two approaches were undertaken. For short-term experiments, mice ($n = 8$ – 10 mice per group) were orally administered a single dose of *InvA*^{2}*Aro*^{2} *Salmonella* and sacrificed at 30, 60, 180 and 270 min postinfection. For long-term experiments, mice received the same dose of *InvA*^{2}*Aro*$^+$ and were sacrificed 5 d postinfection. Tissues (small intestine and Peyer's patches [PPs] for short term experiments; PPs, mesenteric lymph node [MLNs], and spleen for long-term experiments) were harvested, weighed, and treated with gentamicin (1 h at 37°C). After repeated washings in PBS, tissues were homogenized. Serial dilutions of the homogenates were plated on Luria – Bertani agar and incubated overnight at 37°C. To determine Ab responses to noninvasive *Salmonella* strain, mice received three doses of 1×10^8 *InvA*^{2}*AroA*^{2} *S.* Typhimurium at 3-d intervals.

Intravital two-photon microscopy

Intestinal loops were performed as described (5); mice were then placed on a mouse holder; the temperature of the animals was maintained by an enclosed microscope temperature control system (Life Imaging Services, Basel, Switzerland). Two-photon excitation was done with a Chameleon Ultra II Ti:Sapphire laser and Chameleon Compact OPO (Coherent), and the fluorescence emission was measured with four photomultiplier tubes with filters for 420/50, 525/50, 595/40, and 655/40 nm. The microscope system and data acquisition were controlled by Imspector Pro 4.0 software. Image analysis was done with the Fiji/ImageJ package.

Immunofluorescence and transmission electron microscopy

Immunohistochemistry was carried out on 10-μm sections as described in detail elsewhere (14, 15). Briefly, nonspecific binding sites were quenched with 5% BSA; sections were then incubated with rabbit anti-entactin Ab (Abcam, Cambridge, U.K.) followed by Cy5-conjugated anti-rabbit IgG (Jackson ImmunoResearch Laboratories, West Grove, PA) for 45 min. Sections were counterstained with tetramethylrhodamine isothiocyanate – conjugated phalloidin (Sigma-Aldrich) and analyzed with a Zeiss LSM 510 confocal microscope. For transmission electron microscopy (TEM) analysis, samples were processed according to standard procedure (16) and examined with a Philips 201 electron microscope.

Ab responses

S. Typhimurium – specific IgG and IgA were detected in serum and feces. Briefly, serum was obtained after 1 h incubation at 37°C and collected after centrifugation. Fecal samples were weighed and resuspended in PBS in the presence of protease inhibitors; debris-free supernatants were then collected after centrifugation. ELISA plates (Costar) were coated with lysate from wt *S.* Typhimurium obtained as described by others (17). Plates were blocked and then incubated with dilutions of both serum and fecal solution. After washing, plates were incubated with anti-IgA – and anti-IgG – biotinylated Ab (Abcam); this was followed by incubation with streptavidin-peroxidase (Abcam). Also, numbers of single IgA Ab-forming cells (AFCs) were detected using a modified ELISPOT assay developed in our laboratory (18) in 96-well membrane ELISPOT plates (Whatman) coated with lysate from wt *S.* Typhimurium as above.

Flow cytometry and isolation of CX_3CR1^+ cells

Following bacterial challenge, luminal contents were carefully recovered by gently flushing the intestine with PBS. Intraluminal $CX_3CR1^{+/gfp}$ cells were isolated and characterized by flow cytometry as described in detail elsewhere (5). Samples were analyzed by a BD FACSAria II (BD Biosciences). The following Abs were used: CD11c (HL3; BD Biosciences), CD103 (M290; BD Biosciences), CD103 (2E7; eBioscience), F4/80 (BM8; eBioscience), MHC class II (M5/114.15.2; eBioscience), and Siglec-F (E50-2440; BD Biosciences). For the isolation of CX_3CR1^+ cells, intestinal tissues from $CX_3CR1^{+/gfp}$ mice were collected and tissues were repeatedly treated with HBSS containing EDTA (2 mM). After each treatment, tissues were shaken and supernatant was discarded. After each wash an aliquot from the supernatant was analyzed by microscopy to detect the presence of IECs; EDTA treatment was stopped (usually after three to four treatments) when epithelial cells were not present in the supernatant. Tissues were then treated for 50 min in RPMI 1640 with 10% FCS, 0.24 mg/ml collagenase VIII (Sigma-Aldrich), and 40 U/ml DNase I (Roche) as described by others (19); after shaking, cell suspensions were filtered and then purified by gradient separation as described before (5). Cells were sorted (~95% purity), suspended in PBS, and injected into the intestinal lumen for pathogen exclusion assay.

S. Typhimurium exclusion assay

Experiments of adoptive transfer were performed to assess the ability of CX_3CR1 cells to prevent *S.* Typhimurium from traversing the epithelial barrier. $CX_3CR1^{+/gfp}$ and $CX_3CR1^{gfp/gfp}$ mice were used as donors, and gfp-labeled CX_3CR1 cells were isolated as described above. $CX_3CR1^{2/2}$

mice (six mice per group) were used as recipients, and they received a single oral dose of 1 × 10^7 invasive/nonreplicating *InvA*$^+$*AroA*^{2} *S.* Typhimurium ~5 – 10 min after the delivery of a solution of $NaHCO_3$ and then anesthetized. Initially, four groups of mice were used. Group I was injected in the intestinal lumen with 0.5 × 10^3 $CX_3CR1^{+/gfp}$ cells ~10 min after *S.* Typhimurium infection and sacrificed 30 min postinfection; tissues were then removed, washed, and homogenates were plated on Luria – Bertani agar. Group II received the same number of $CX_3CR1^{+/gfp}$ cells after 10 min; subsequently, the number of intraluminal $CX_3CR1^{+/gfp}$ cells was increased to 1 × 10^4 with a second injection 30 min postinfection. Mice were sacrificed 90 min after the initial *S.* Typhimurium infection and tissues were treated as for group I. In group III, mice received a total of 4.5 × 10^4 *S.* Typhimurium in three injections administered 10, 30, and 90 min postinfection. This group of mice was sacrificed and tissue removed 120 min postinfection. Group IV was treated as group I, with the difference that the mice received 1 × 10^4 $CX_3CR1^{+/gfp}$ cells after 10 min; mice were sacrificed 30 min postinfection. At each injection cells were equally divided into two injection sites ~1 and 3 cm from the pylorus. The same protocol was repeated in an additional four groups of $CX_3CR1^{2/2}$ mice (V – VIII) that received adoptive transfer of $CX_3CR1^{gfp/gfp}$ cells.

Permeability assay

Intestinal permeability to soluble (dextran) and particulate Ag (polystyrene microparticles) was measured in 6- to 8-wk-old $CX_3CR1^{gfp/gfp}$, $CX_3CR1^{+/gfp}$, and syngeneic wt mice (four mice per group). FITC-labeled dextran (FD4; Sigma-Aldrich) was dissolved in PBS at a concentration of 100 mg/ml and administered to each mouse (44 mg/100 g body weight) by oral gavage. Blood samples were collected after 6 h and the plasma was analyzed for FD4 concentration using a fluorescence spectrometer at an excitation wavelength of 490 nm and emission wavelength of 520 nm. Intestinal transport of polystyrene particles (Fluoresbrite YG carboxylate microspheres, 0.50 μm) was assessed as described in detail elsewhere (20).

Statistical analysis

Data are expressed as mean ± SD, and statistical comparisons were made by the Student unpaired *t* test. The *p* values were considered significant at $p < 0.05$.

Results

Bacteria translocation is increased in mice lacking intraluminal migration of CX_3CR1^+ cells but not Ag sampling via the indirect route

Translocation of *InvA*^{2} *S.* Typhimurium was investigated in $CX_3CR1^{2/2}$ mouse strains either able (C57BL/6) (8) or unable ($CX_3CR1^{2/2}$ or BALB/c) to sample luminal bacteria via the indirect route (6, 10) (Supplemental Fig. 1). Following oral delivery of *InvA*^{2} *S.* Typhimurium, Ag sampling-competent/migration-competent C57BL/6 mice and sampling-deficient/migration-competent BALB/c mice had similar numbers of *S.* Typhimurium penetrating both the conventional epithelium of the small intestine and the specialized follicle-associated epithelia of PPs (Fig. 1A, 1B) at any time point during the initial stages of the infection. In contrast, sampling-deficient/migration-deficient $CX_3CR1^{2/2}$ mice showed significantly higher numbers of bacteria after 30 and 60 min postinfection within the PPs and the small intestinal lamina propria that remained significantly higher throughout the experiment. Additionally, the number of replicating *InvA*^{2}*AroA*$^+$ *S.* Typhimurium recovered from PPs, MLNs, and spleen 5 d after oral delivery was higher in $CX_3CR1^{2/2}$ mice compared with their wt counterparts (Fig. 1C). Increased bacterial translocation across the gut epithelium in CX_3CR1-deficient mice (both $CX_3CR1^{2/2}$ and $CX_3CR1^{gfp/gfp}$) was not the result of increased permeability of the epithelial barrier, as shown by using soluble tracer and microparticles (Fig. 2). Indeed, serum levels of orally delivered fluorescent FITC-dextran (Fig. 2A) and numbers of orally delivered FITC-labeled latex microparticles (Fig. 2B) were similar to those in wt mice. Increased bacterial transport in the gut of $CX_3CR1^{gfp/gfp}$ mice was also seen following infection with *InvA*$^+$ *S.* Typhimurium. Confirming a previous report (6), $CX_3CR1^{gfp/gfp}$ mice succumbed 7 d after oral delivery of a lethal dose of invasive *S.* Typhimurium at a significantly

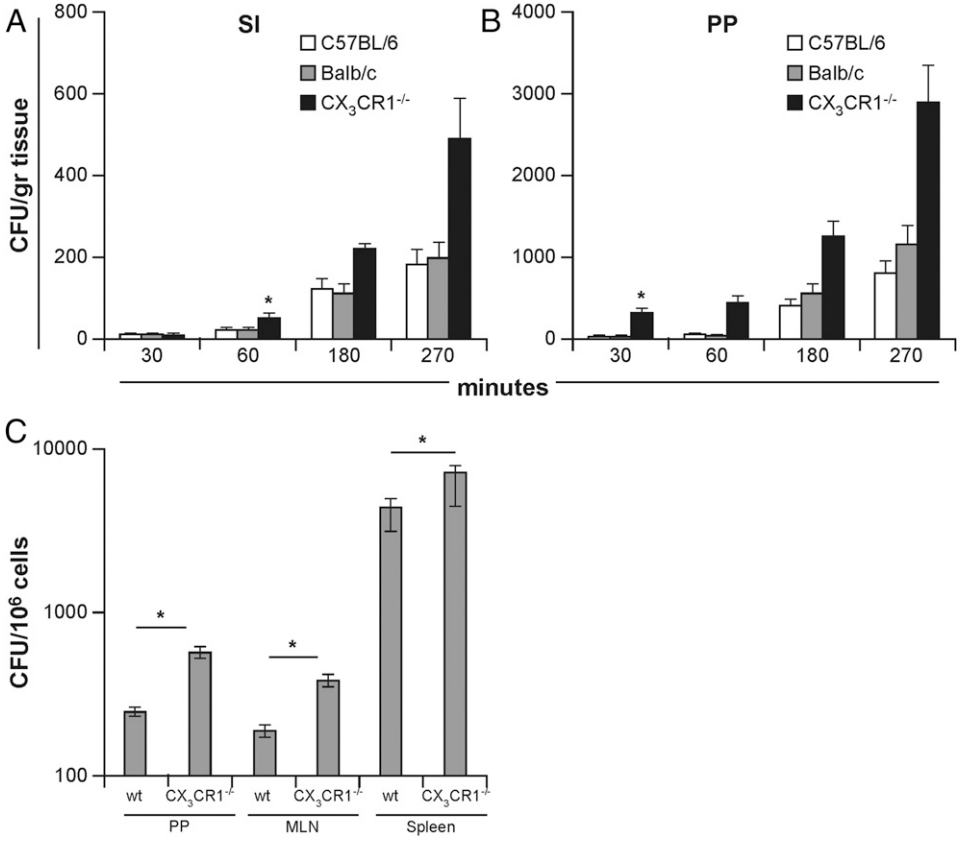

FIGURE 1. Role of CX_3CR1-mediated sampling and migration in the uptake of noninvasive *InvA*^{2} *S.* Typhimurium. Numbers of *S.* Typhimurium traversing the conventional (**A**) (small intestine [SI]) and specialized (**B**) (PPs) epithelia did not differ in mouse strains that have been shown to be either sampling competent/migration competent (C57BL/6) or sampling deficient/migration competent (BALB/c). In contrast, *S.* Typhimurium uptake was significantly higher in $CX_3CR1^{2/2}$ mice that were both sampling deficient and migration deficient (eight mice per group). Similarly, (**C**) higher numbers of *S.* Typhimurium were found to be higher in the GALT (PP and MLN) and spleen of $CX_3CR1^{2/2}$ mice compared with wt mice (10 mice per group), 6 d after a single oral delivery of noninvasive-replicating *InvA*^{2}*Aro*$^+$ *S.* Typhimurium. *$p < 0.05$.

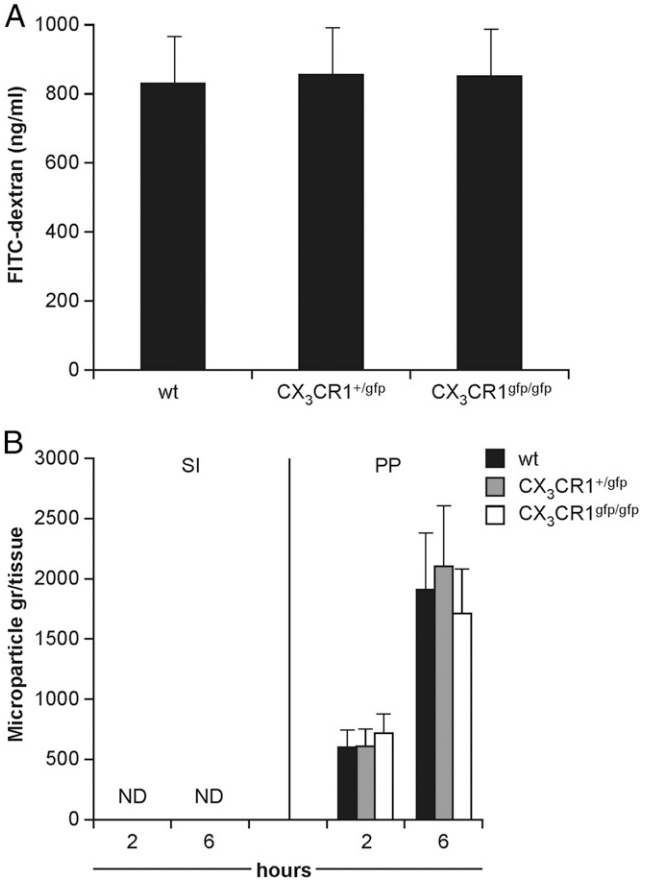

FIGURE 2. Intestinal permeability in CX_3CR1-deficient mice. Oral delivery of a single dose of either FITC-dextran (**A**) or yellow-green fluorescent polystyrene microparticles (**B**) showed that intestinal permeability to both soluble and particulate tracers was not affected by the lack of functional fraktalkine receptor (four mice per group). This demonstrates that the higher bacterial load in the intestine as shown in Fig. 1 could not be attributed to an intrinsic "leaky" gut in $CX_3CR1^{2/2}$ mice. *p , 0.05.

faster rate compared with their $CX_3CR1^{+/gfp}$ counterparts (Supplemental Fig. 2A) and showed higher bacterial load in their organs (Supplemental Fig. 2B). Also, to rule out that some effects of CX_3CR1 deficiency on bacterial translocation might be related to altered activation of adaptive immune responses, we assessed bacterial translocation in $CX_3CR1^{+/2}$ and $CX_3CR1^{2/2}$ mice on the $RAG^{2/2}$ background. We observed that the $RAG^{2/2}$ background did not affect bacterial translocation (Supplemental Fig. 2C). These results taken together would suggest that Ag sampling via the indirect route does not play a significant role in *S.* Typhimurium uptake, at least at the initial stage of infection; instead, it appeared that the lack of ***Salmonella***-induced CX_3CR1^{+} cell intraluminal migration favored bacterial translocation.

Intraluminal cell migration is triggered by epithelium-derived signals, and it is higher in response to invasive S. *Typhimurium*

The potential critical role of intraluminal CX_3CR1^{+} cells in controlling pathogen uptake prompted us to investigate this event in detail. First, we determined whether ***Salmonella***-induced CX_3CR1^{+} cell migration was abolished or simply delayed in CX_3CR1-deficient mice. After the introduction of ***InvA*** ^{2} *S.* Typhimurium into isolated intestinal loops of $CX_3CR1^{+/gfp}$ mice, the number of CX_3CR1^{+} cells appearing in the gut lumen 30 min postinfection (Fig. 3A) reached $0.71 \times 10^4 \pm 1.2 \times 10^3$, which was approximately ~30-fold higher than levels seen in $CX_3CR1^{gfp/gfp}$ mice ($1.3 \times 10^2 \pm 1 \times 10^2$). The numbers of intraluminal CX_3CR1^{+} cells increased steadily between 90 and 270 min, reaching $8.9 \times 10^4 \pm 5 \times 10^3$. In contrast, no increase in the number of intraluminal CX_3CR1^{+} cells was observed in $CX_3CR1^{gfp/gfp}$ mice at any time point after infection, showing that migration is completely abolished in mice lacking a functional fractalkine receptor. Furthermore, we assessed the role of epithelium-derived signals in the migration of CX_3CR1^{+} cells in response to *S.* Typhimurium. To this end, $MyD88^{\Delta IEC}$ mice that lacked the adaptor molecule MyD88 solely in the IECs were challenged with *S.* Typhimurium. The migration was completely suppressed in $MyD88^{\Delta IEC}$ mice compared with syngeneic wt counterparts ($1.5 \times 10^2 \pm 1 \times 10^2$ and $6.5 \times 10^4 \pm 1.1 \times 10^4$, respectively, at 5 h postinfection) (Fig. 3B), thus showing that signals from IEC-associated TLRs are the triggering event. We then evaluated the migration of CX_3CR1^{+} cells in response to oral delivery of *S.* Typhimurium strains that differed in their capacity to invade the host. Intraluminal migration in $CX_3CR1^{+/gfp}$ mice (Fig. 3C) was significantly higher after infection with the invasive *S.* Typhimurium strain ($4.3 \times 10^2 \pm 1.2 \times 10^2$) compared with noninvasive strain ($2.1 \times 10^2 \pm 1 \times 10^2$) already within 30 min postinfection. The number of intraluminal cells steadily increased with time and, after 5 h, it reached $4.4 \times 10^4 \pm 9 \times 10^3$ and $1.7 \times 10^4 \pm 1.2 \times 10^3$ cells for invasive and noninvasive *S.* Typhimurium, respectively. Migration was significantly reduced in response to both *S.* Typhimurium variants at 12 h postinfection, consistent with intraluminal migration of CX_3CR1^{+} cells being restricted to the initial stage of infection. We previously reported that CX_3CR1^{+} cells were the only intraluminal cell population harboring intracellular *S.* Typhimurium shortly after infection (5), suggesting a possible role in ***Salmonella*** exclusion. In agreement with this interpretation, we observed that at 5 h postinfection migration-competent $CX_3CR1^{+/gfp}$ mice had a significantly higher fecal (excluded) bacteria load compared with migration-deficient $CX_3CR1^{gfp/gfp}$ mice (Fig. 3D).

Salmonella-*induced migration of* CX_3CR1^{+} *cells occurred through paracellular channels in the epithelium*

Then, intravital two-photon microscopy was used to study in detail the transepithelial migration of CX_3CR1^{+} cells in $CX_3CR1^{+/gfp}$ mice shortly (3 h) after the introduction of ***InvA*** ^{2} *S.* Typhimurium into isolated ileal loops. First, the still image (orthogonal cross-sections through the three-dimensional stacks in successive time frames) (Fig. 4A-E) of the in vivo real-time video (Supplemental Video 1) showed a fluorescent $CX_3CR1^{+/gfp}$ cell protruding into the intestinal lumen from the surface of the intestinal epithelium (Fig. 4A) and progressed farther into the lumen (Fig. 4B, 4C) before moving away from the entry site (Fig. 4D, 4E). It also appeared that the imaged cell was immediately followed by another $CX_3CR1^{+/gfp}$ cell migrating via the same opening in the epithelium (Fig. 4D, 4E, Supplemental Video 1). This migratory pattern was also investigated by both immunohistochemistry (Fig. 4F) and TEM (Fig. 4G, 4H). Fig. 4G also showed three cells migrating (mC1-3) in single file through the paracellular channel into the lumen, one of which (mC2) was in close contact with *S.* Typhimurium (Fig. 4H). The migration of CX_3CR1^{+} cell is unidirectional; after collecting intraluminal $CX_3CR1^{+/gfp}$ cells and reintroducing them into freshly isolated intestinal ileal loop, we never observed $CX_3CR1^{+/gfp}$ cells traversing the epithelial barrier to migrate back into the intestinal tissue. Most intraluminal $CX_3CR1^{+/gfp}$ cells (Fig. 5) at 5 h postinfection displayed the phenotype of gut-resident macrophages (MHC class $II^{+}F4/80^{+}CD11c^{+}CD103^{2}Siglec\text{-}F^{2}$) that in steady-state situations do not migrate to MLN, display poor T cell stimulatory capability, and possess high phagocytic activity both in vitro and in vivo (19, 21).

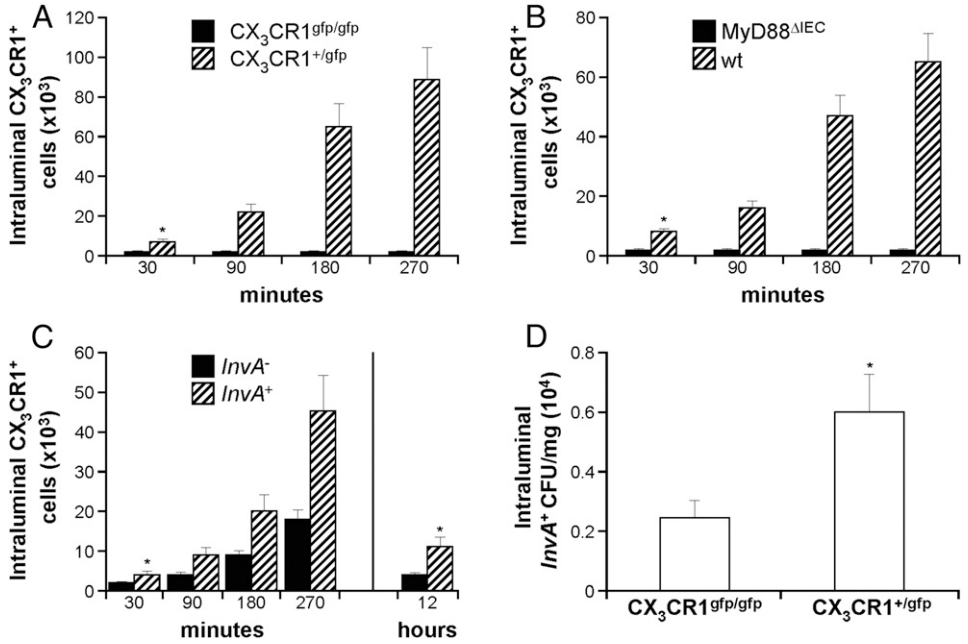

FIGURE 3. Regulation of *S.* Typhimurium–induced migration of CX_3CR1^+ cells. The role of the fraktalkine CX_3CR1 receptor in *S.* Typhimurium-induced migration was assessed in mice with a functional ($CX_3CR1^{+/gfp}$) or nonfunctional ($CX_3CR1^{gfp/gfp}$) receptor. Intraluminal migration of CX_3CR1^+ cells was absent in CX_3CR1-deficient mice (A) (seven to eight mice per group) that had been challenged with 1×10^7 *InvA*^{2} *S.* Typhimurium. The lack of the fraktalkine receptor completely abolished, and did not simply delay, the pathogen-induced migration. IEC-derived signals are required for CX_3CR1^+ cell recruitment and migration; *S.* Typhimurium–dependent intraluminal recruitment of CX_3CR1^+ cells was also absent in mice with a target deletion of MyD88 in the IEC ($MyD88^{\Delta IEC}$ mice) (B) (five to six mice group). In (C) it is shown that intraluminal migration is significantly more pronounced in response to oral challenge (1×10^7) with invasive (*InvA*$^+$) *Salmonella* variant. Migration appeared to be restricted at the initial stage of infection and it declined significantly 12 h postinfection for both invasive and noninvasive strains. The presence of intraluminal CX_3CR1^+ cells led to a significant increase in fecal bacterial load (D) compared with $CX_3CR1^{gfp/gfp}$ mice 5 h after oral delivery of invasive *S.* Typhimurium as in (C). $*p < 0.05$.

Lack of CX_3CR1-mediated sampling did not affect Ab responses to S. *Typhimurium*

It has been suggested that Ag sampling mediated by CX_3CR1^+ cells in the lamina propria, also called the indirect route (22), plays a significant role in the generation of mucosal and systemic immune responses. However, direct evidence of this was still lacking. Thus, we assessed mucosal and systemic Ab responses to *InvA*^{2}*AroA*^{2} *S.* Typhimurium that specifically target the CX_3CR1-mediated entry route (22) in $CX_3CR1^{gfp/gfp}$ mice that lack a functional CX_3CR1 receptor. We observed that the levels of serum IgG were consistently higher in $CX_3CR1^{gfp/gfp}$ mice compared with $CX_3CR1^{+/gfp}$ mice starting at week 2 postinfection (Fig. 6A), although it did not reach statistical significance. Instead, sIgA production in $CX_3CR1^{gfp/gfp}$ mice, albeit significantly lower than the one induced by invasive/nonreplicating *InvA*$^+$*AroA*^{2} *S.* Typhimurium (data not shown), was significantly higher compared with wt mice (Fig. 6B) starting from week 3 postinfection. The higher *S.* Typhimurium–specific IgA response in $CX_3CR1^{gfp/gfp}$ mice was confirmed by assessing the numbers of AFCs in the PPs (Fig. 6C).

The presence of CX_3CR1^+ cells in the intestinal lumen significantly reduced the number of S. *Typhimurium penetrating the epithelial barrier*

Finally, we tested the hypothesis that intraluminal CX_3CR1^+ cells contributed to immune exclusion of *S.* Typhimurium. At various intervals, shortly following oral delivery of 1×10^7 *InvA*$^+$*AroA*^{2} *S.* Typhimurium, CX_3CR1^+ cells isolated from $CX_3CR1^{+/gfp}$ donors were injected into the intestinal lumen of migration-deficient $CX_3CR1^{2/2}$ mice (details of protocol are shown in Supplemental Fig. 3). Four groups of mice were used, and the number of adoptively transferred cells at any given time point was based on a time course experiment carried out previously (Fig. 3C). The adoptive transfer of intraluminal CX_3CR1^+ cells in $CX_3CR1^{2/2}$ mice significantly reduced the number of *InvA*$^+$ *S.* Typhimurium traversing the epithelial barrier (Fig. 7A). In the presence of 0.5×10^3 CX_3CR1^+ cells, the number of tissue CFU of *InvA*$^+$ *S.* Typhimurium declined (from 1.2×10^3 to 3.3×10^2 to 2.1×10^2 to 1.4×10^2) at 30 min postinfection (group I). Similarly, significant reductions in bacterial load in the intestinal tissues were observed in groups II and III. Finally, group IV was passively transferred 15 min after *S.* Typhimurium administration with a number of CX_3CR1^+ cells (1×10^4) that far exceeded the number of CX_3CR1^+ cells found in the small intestine at the beginning of the infection. In this case, the presence of intraluminal CX_3CR1^+ cells almost completely abolished *Salmonella* invasion of intestinal tissue (CFU tissue > 40). Importantly, when $CX_3CR1^{gfp/gfp}$ mice were used in experiments of adoptive transfer (Fig. 7B), we observed that these cells afforded a similar level of protection against *S.* Typhimurium invasion compared with $CX_3CR1^{+/gfp}$ cells. This demonstrated that transepithelial migration and no other intrinsic defects of $CX_3CR1^{2/2}$ cells is the critical event in immune exclusion against *S.* Typhimurium. Taken together, these results demonstrated that CX_3CR1^+ cells that migrate rapidly into the lumen represented a rapidly deployed protective response that prevents harmful microbes such as *S.* Typhimurium from infecting the host.

Discussion

The presence of epithelial tight junctions, a thick layer of mucus, and secretion of sIgA ensures that harmful microorganisms do not breach the intestinal epithelium. In this study, we demonstrated that when this barrier is breached by invading pathogenic bacteria the host rapidly responds by sending into the intestinal lumen pathogen (*S.* Typhimurium)–capturing CX_3CR1^+ cells to limit the number

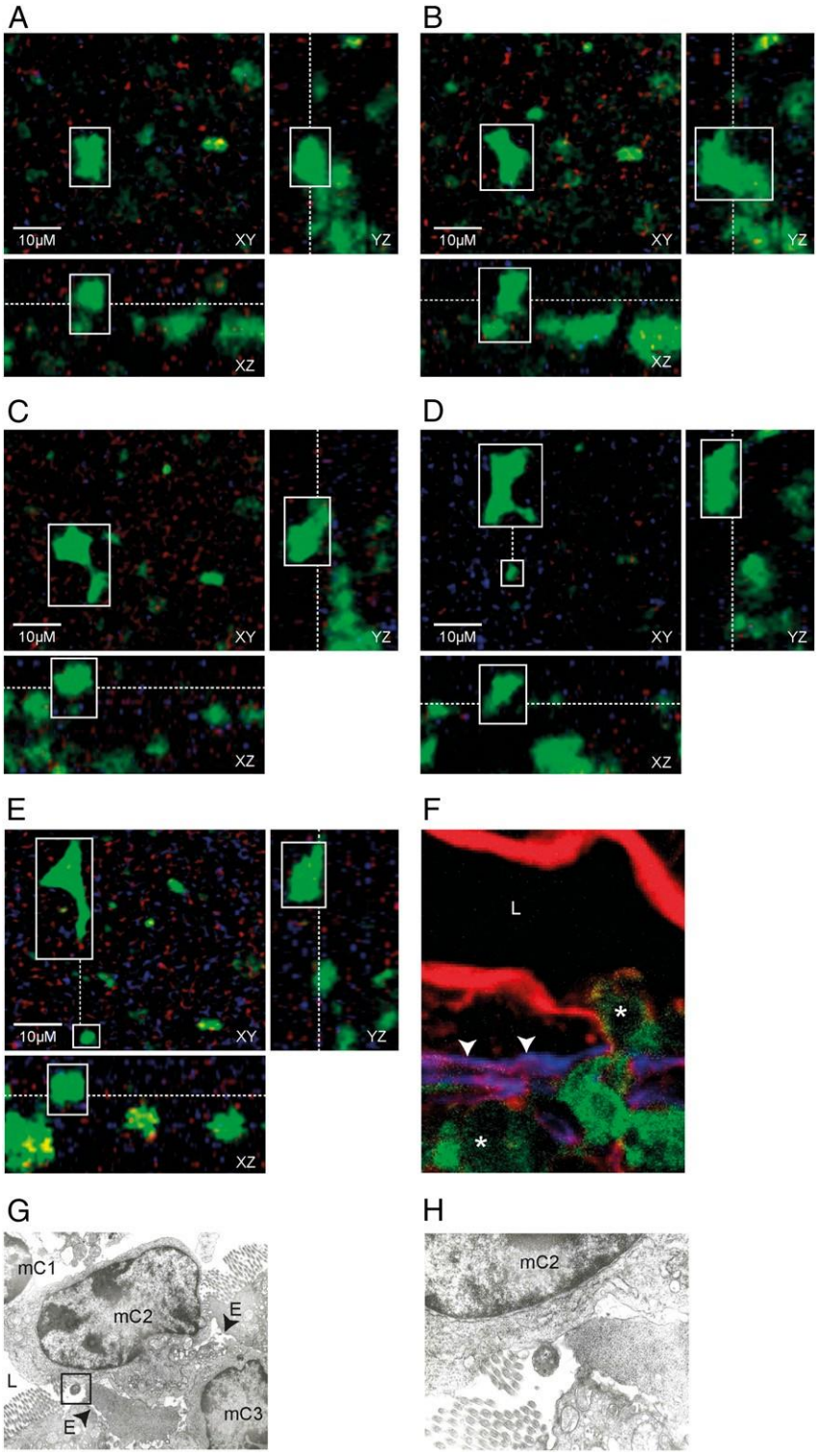

FIGURE 4. CX_3CR1^+ cell passage into the intestinal lumen occurred through paracellular spaces. Still images are from in vivo real-time video (Supplemental Video 1): images are of orthogonal cross-sections through the three-dimensional stacks in successive time frames. Detailed views show the movement of a fluorescent $CX_3CR1^{+/gfp}$ cell following challenge with ***Salmonella***. In (**A**), the $CX_3CR1^{+/gfp}$ cell (white box) is protruding from the epithelial surface; the outward movement is more pronounced in (**B**). In (**C**), the migrating cell keeps protruding into the lumen until it completed its migration and moved away (dotted line) from the entry site (small white box) (**D** and **E**). The migrating cell is immediately followed by another $CX_3CR1^{+/gfp}$ cell protruding into the lumen from the same opening [(**D**) and (**E**), small white box]. Images on the *y,z* plan (**A**–**E**) show that once into the lumen the cell progresses in a nonlinear (side-to-side) pattern on the epithelial surface. Scale bars, 10 *m*m. The migration pattern was further investigated by immunofluorescence microscopy (**F**) and TEM (**G** and **H**). In (**F**), $CX_3CR1^{+/gfp}$ cells (asterisks) migrate into the intestinal lumen (L) across the basal membrane (arrowheads), identified by anti-entactin Ab (blue) and then the epithelium identified with phalloidin (red). In (**G**) and (**H**), a series of cells (mC1 – 3) moved into the lumen (L) via the paracellular space (arrowheads) between adjacent enterocytes (**E**) through the same paracellular channel. Also, in (**G**) one migrating cell (mC2) is in close contact with ***Salmonella*** (box) (detail in **H**).

of bacteria penetrating the epithelial barrier. The rapid migration is triggered by the initial interaction of pathogens with IECs because this migration is absent in mice lacking the adaptor molecule MyD88 solely within the epithelium. The interaction of *S.* Typhimurium and the IEC-associated TLR may lead to two different events. CX_3CR1^+ cells can directly sample bacteria and shuttle them across the epithelium (6); alternatively, these cells could also move through the epithelium and migrate into the lumen where they capture *S.* Typhimurium (5).

However, although it was suggested that CX_3CR1 sampling was relevant to mounting Ag-specific responses, the role and biological relevance of the rapid migration of *S.* Typhimurium – capturing CX_3CR1^+ cells in the lumen remained to be determined. CX_3CR1-mediated sampling and migration showed significant differences. The most notable difference was that although CX_3CR1 migration in response to *S.* Typhimurium takes place irrespective of the mouse strain, such as C57BL/6 and BALB/c (5), the ability to sample luminal bacteria via the indirect route may or may not be possible according to the genetic makeup of the host (7, 8, 10), an observation that led to the conclusion that CX_3CR1-mediated sampling is not a universal phenomenon (23). We exploited this feature to investigate the biological relevance of these two CX_3CR1-mediated

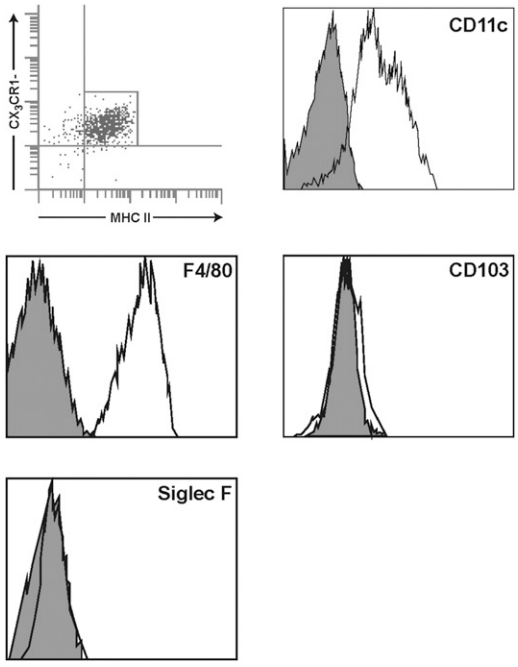

FIGURE 5. Phenotypic analysis of intraluminal CX_3CR1^+ cell population. Flow cytometry analysis of intraluminal cells in $CX_3CR1^{+/gfp}$ (BALB/c background) 5 h following intestinal challenge with 1 × 10^7 *InvA*^{2} *Salmonella*. The vast majority of the cell population rapidly recruited into the intestinal lumen showed the phenotype of resident (stationary) macrophages with poor T cell stimulatory activity and high phagocytic activity. These cells were $CD11C^+F4/80^+$MHC class II^+ but did not express the canonical marker for gut-derived dendritic cells, CD103; also, these cells lacked the neutrophil marker Siglec-F.

events during the initial stage of *S.* Typhimurium infection. We observed that despite lacking the ability to sample bacteria via the indirect route, BALB/c mice showed very similar intestinal uptake of noninvasive *S.* Typhimurium, which specifically targets the indirect route compared with sampling-competent wt C567BL/6 mice. This observation is of particular relevance when examined in the context of *S.* Typhimurium uptake in CX_3CR1-deficient mice that lacked both CX_3CR1 sampling (6) and intraluminal migration (9). We observed that CX_3CR1-deficient mice showed a significantly higher bacterial load both at the mucosal level and systemically compared with both C57BL/6 and BALB/c mice. Increased pathogen uptake in CX_3CR1-deficient mice did not depend on intrinsic alteration of the integrity of the epithelial barrier in both $CX_3CR1^{2/2}$ and $CX_3CR1^{gfp/gfp}$ mice because permeability to either soluble or particulate tracers was similar to what was observed in their wt counterparts. Overall, these results suggest that sampling via the indirect route does not play a significant role in *S.* Typhimurium uptake through the intestinal epithelium, at least during the early stage of infection. Instead, they point to the lack of rapid intraluminal migration of CX_3CR1^+ cells as the critical factor favoring bacterial translocation. This hypothesis is further strengthened by the observation that intraluminal migration of CX_3CR1^+ cells in $CX_3CR1^{+/gfp}$ mice was associated with increased fecal bacterial counts compared with migration-deficient $CX_3CR1^{gfp/gfp}$ mice. Importantly, others have shown that $CX_3CR1^{2/2}$ mice displayed increased translocation of commensal bacteria to MLN (24), thus suggesting that intraluminal migration of CX_3CR1^+ cells might also play a role in controlling the access of commensal microbes to the intestinal tissue. Furthermore, CX_3CR1-deficient mice are more susceptible to *S.* Typhimurium infection, as seen by us and others (6); however, the reason for this remained to be determined. One possibility was that the lack of CX_3CR1-mediated sampling led to an impaired immunity to *S.* Typhimurium. We observed that CX_3CR1-deficient mice developed a systemic IgG response comparable to wt control and, surprisingly, a significantly higher intestinal Ab response (IgA) to a noninvasive *S.* Typhimurium that targets the indirect route and is characterized by poor mucosal antigenic properties (22). It is likely that the latter observation could be attributed to the higher number of *S.* Typhimurium reaching the PPs, the inductive sites of IgA-mediated immunity, in CX_3CR1-deficient mice. Taken together, these results strongly suggested that increased susceptibility to *S.* Typhimurium infection in CX_3CR1-deficient mice was due, at least partly, to the lack of protection afforded by CX_3CR1-mediated pathogen exclusion in the early stage of infection.

As a parallel observation, these data also confirmed previous reports suggesting that the *S.* Typhimurium type III secretion system (*InvA*) facilitates uptake by follicle-associated epithelia

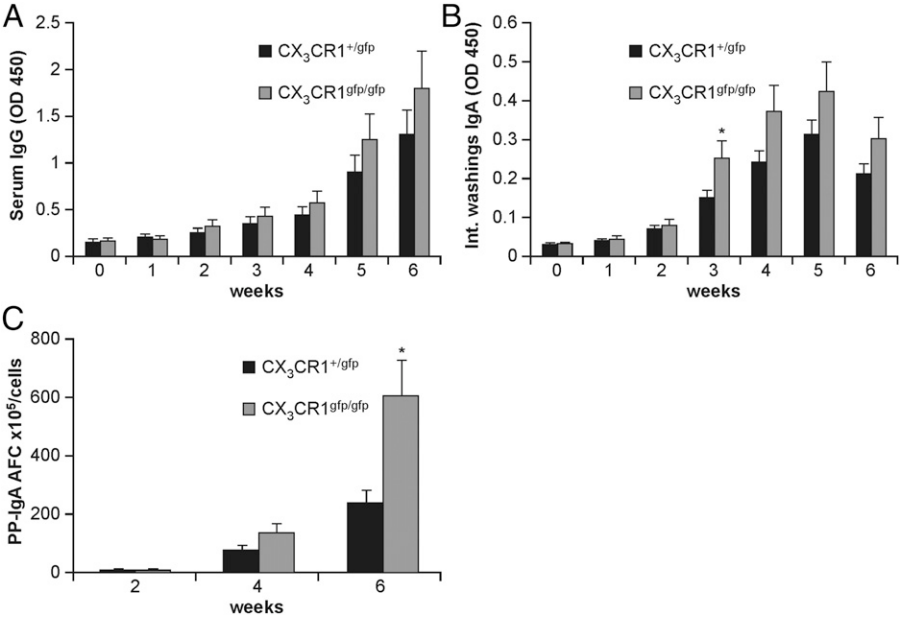

FIGURE 6. Humoral immunity to noninvasive *Salmonella* in $CX_3CR1^{2/2}$ mice. Mice (9 – 10 mice per group) received three consecutive doses of 1 × 10^7 of noninvasive/nonreplicating *InvA*^{2}*AroA*^{2} *Salmonella* at 3-d intervals. Levels of serum IgG (A) and intestinal IgA (B) *Salmonella*-specific Abs were determined by ELISA. Both responses appeared to be higher in $CX_3CR1^{gfp/gfp}$ compared with $CX_3CR1^{+/gfp}$ mice, although only intestinal levels of IgA were significantly different starting from week 3 postinfection. Higher mucosal IgA immunity in $CX_3CR1^{gfp/gfp}$ mice was further confirmed by monitoring numbers of AFCs in PPs at weeks 2, 4, and 6 postinfection (C). *p , 0.05.

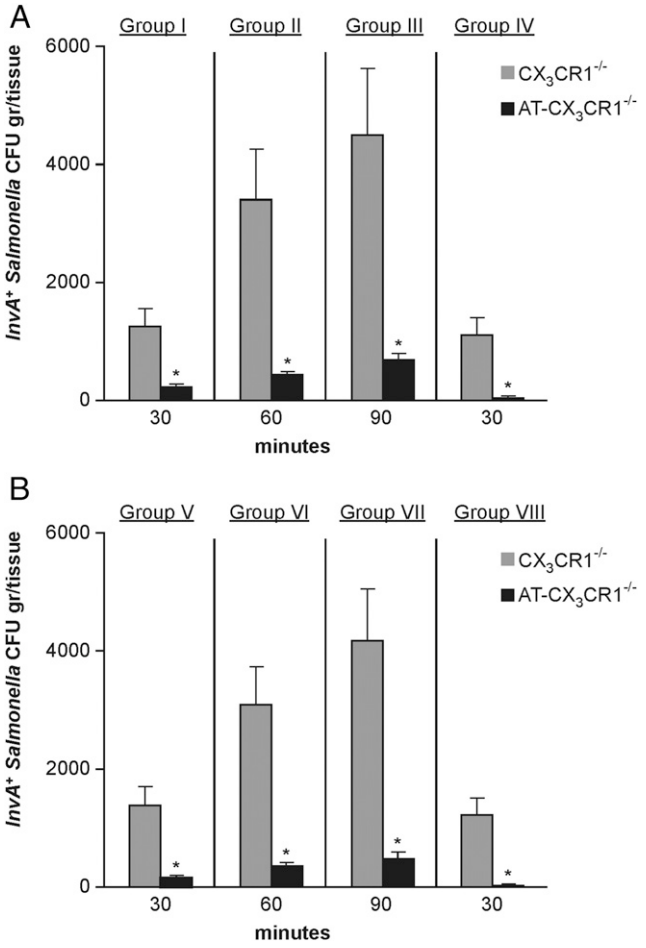

FIGURE 7. CX_3CR1^+ cell–mediated pathogen exclusion. $CX_3CR1^{2/2}$ mice (six mice per group) were infected with a single oral dose (1×10^7) of invasive/nonreplicating *InvA*$^+$*Aro*^{2} *Salmonella*. *Salmonella* infecting the intestinal tissue was determined in the absence ($CX_3CR1^{2/2}$, gray bars) or presence (AT-$CX_3CR1^{2/2}$, black bars) of $CX_3CR1^{+/gfp}$ (A) or $CX_3CR1^{gfp/gfp}$ (B) cells that were adoptively transferred directly into the intestinal lumen. A significant decline of *S.* Typhimurium CFU per gram per tissue was observed in group I (A) 30 min postinfection following adoptive transfer of 0.5×10^3 $CX_3CR1^{+/gfp}$ cells. Significant reduction in the number of pathogens invading the host was also seen in groups II and III that received increasing numbers of CX_3CR1^+ that were determined according to the time course study shown in Fig. 3C. In group IV, the introduction in the lumen of a larger, nonphysiologically high number of intraluminal CX_3CR1^+ cells (1×10^4) or higher (20-fold increase compared with the number of cells usually found in the gut 15 min postinfection) nearly completely abolished *S.* Typhimurium infection. A similar pattern was observed in parallel experiments when $CX_3CR1^{gfp/gfp}$ cells were used for the adoptive transfer (groups V–VIII) (B), showing that the lack of transepithelial migration, and no other intrinsic defects of $CX_3CR1^{2/2}$ cells, is critical for immune exclusion of *S.* Typhimurium. $^*p < 0.05$.

microfold cells, but its absence does not totally compromise the ability of *S.* Typhimurium to target this entry route (25, 26). Intraluminal migration of CX_3CR1^+ cells is unidirectional, and once into the lumen they do not traverse back to the intestinal epithelium. Determining the fate of intraluminal *S.* Typhimurium–capturing CX_3CR1^+ cells was prompted by the important finding that in mice *Toxoplasma gondii*–infected neutrophils that had migrated into the intestinal lumen during infection can move back into the intestinal tissue at a later stage (1 wk postinfection) (27). The observation that $CX_3CR1^{+/gfp}$ in contrast to infected neutrophils undertake a one-way journey suggested that neutrophils may be intrinsically different from CX_3CR1^+ cells in their ability to traverse back to the epithelium. Alternatively, it is possible that in contrast to *S.* Typhimurium, *T.* gondii might trigger the secretion/expression of cytokine/surface molecules in infected cells that favor this event. Finally, we demonstrated that the migration of CX_3CR1^+ cells into the lumen very early during *S.* Typhimurium infection contributed substantially to pathogen exclusion. Direct introduction of these cells into the lumen of migration-deficient $CX_3CR1^{2/2}$ mice shortly after oral delivery of invasive *S.* Typhimurium significantly reduced the number of pathogens traversing the epithelial barrier. Furthermore, although at this time we cannot rule out the possibility that other cell types may participate in this protective response at a later stage in infection, the previous observation that CX_3CR1^+ cells were the only intraluminal cell population harboring intracellular *S.* Typhimurium (5) implied that these cells are the main player in the exclusion of *S.* Typhimurium in the very early stage of infection. A previous study showed that intraluminal CX_3CR1^+ cells internalized *S.* Typhimurium (5); thus, intracellular killing is the most likely mechanism underlying *S.* Typhimurium exclusion in the gut, although at present other mechanisms such as production of antimicrobial products cannot be ruled out.

At this time, we propose that the CX_3CR1-mediated pathogen exclusion is part of a defensive strategy that includes multiple effector mechanisms acting synergistically. First, the mucous and IgA that are constantly produced in large amounts in the gut provide a preventive barrier that in a steady-state situation controls and limits the access of microbes to the intestinal epithelium. When this defensive barrier is breached, IEC-derived signals readily trigger the intraluminal migration of CX_3CR1^+ cells that are present in large numbers in the subepithelial area where they form an intricate cell network (19, 21). This strategy, implemented in the initial stage of the infection, blocks further pathogen penetration and, in so doing, may prevent the onset of infection by limiting the number of the offending pathogens that can trespass the epithelial barrier. At a later stage this strategy is followed, if necessary, by an additional defensive mechanism represented by the NAIP/NLRC4 inflammasome-mediated expulsion of infected enterocytes (4) to restrict/control *S.* Typhimurium replication/colonization.

Acknowledgments

We thank P. Mastroeni and D. Pickard for *S.* Typhimurium strains, O. Pabst and A. Mowat for $CX_3CR1^{gfp/gfp}$ mice, and K. Hughes for $MyD88^{\Delta IEC}$ mice. We also thank A. Walker and P. Pople for computer artwork and R. Gichev for technical help.

Disclosures

The authors have no financial conflicts of interest.

References

1. Turner, J. R. 2009. Intestinal mucosal barrier function in health and disease. ***Nat. Rev. Immunol.*** 9: 799–809.
2. Mantis, N. J., N. Rol, and B. Corthésy. 2011. Secretory IgA's complex roles in immunity and mucosal homeostasis in the gut. ***Mucosal Immunol.*** 4: 603–611.
3. Johansson, M. E., D. Ambort, T. Pelaseyed, A. Schütte, J. K. Gustafsson, A. Ermund, D. B. Subramani, J. M. Holmén-Larsson, K. A. Thomsson, J. H. Bergström, et al. 2011. Composition and functional role of the mucus layers in the intestine. ***Cell. Mol. Life Sci.*** 68: 3635–3641.
4. Sellin, M. E., A. A. Müller, B. Felmy, T. Dolowschiak, M. Diard, A. Tardivel, K. M. Maslowski, and W. D. Hardt. 2014. Epithelium-intrinsic NAIP/NLRC4 inflammasome drives infected enterocyte expulsion to restrict ***Salmonella*** replication in the intestinal mucosa. ***Cell Host Microbe*** 16: 237–248.
5. Arques, J. L., I. Hautefort, K. Ivory, E. Bertelli, M. Regoli, S. Clare, J. C. Hinton, and C. Nicoletti. 2009. ***Salmonella*** induces flagellin- and MyD88-dependent migration of bacteria-capturing dendritic cells into the gut lumen. ***Gastroenterology*** 137: 579–587, 587.e1–587.e2.

6. Niess, J. H., S. Brand, X. Gu, L. Landsman, S. Jung, B. A. McCormick, J. M. Vyas, M. Boes, H. L. Ploegh, J. G. Fox, et al. 2005. CX_3CR1-mediated dendritic cell access to the intestinal lumen and bacterial clearance. ***Science*** 307: 254 – 258.
7. Rescigno, M., M. Urbano, B. Valzasina, M. Francolini, G. Rotta, R. Bonasio, F. Granucci, J. P. Kraehenbuhl, and P. Ricciardi-Castagnoli. 2001. Dendritic cells express tight junction proteins and penetrate gut epithelial monolayers to sample bacteria. ***Nat. Immunol.*** 2: 361 – 367.
8. Chieppa, M., M. Rescigno, A. Y. Huang, and R. N. Germain. 2006. Dynamic imaging of dendritic cell extension into the small bowel lumen in response to epithelial cell TLR engagement. ***J. Exp. Med.*** 203: 2841 – 2852.
9. Nicoletti, C., J. L. Arques, and E. Bertelli. 2010. CX_3CR1 is critical for Salmonella-induced migration of dendritic cells into the intestinal lumen. ***Gut Microbes*** 1:131 – 134.
10. Vallon-Eberhard, A., L. Landsman, N. Yogev, B. Verrier, and S. Jung. 2006. Transepithelial pathogen uptake into the small intestinal lamina propria. ***J. Immunol.*** 176: 2465 – 2469.
11. Jung, S., J. Aliberti, P. Graemmel, M. J. Sunshine, G. W. Kreutzberg, A. Sher, and D. R. Littman. 2000. Analysis of fractalkine receptor CX_3CR1 function by targeted deletion and green fluorescent protein reporter gene insertion. ***Mol. Cell. Biol.*** 20: 4106 – 4114.
12. Skoczek, D. A., P. Walczysko, N. Horn, A. Parris, S. Clare, M. R. Williams, and A. Sobolewski. 2014. Luminal microbes promote monocyte-stem cell interactions across a healthy colonic epithelium. ***J. Immunol.*** 193: 439 – 451.
13. Rowley, G., H. Skovierova, A. Stevenson, B. Rezuchova, D. Homerova, C. Lewis, A. Sherry, J. Kormanec, and M. Roberts. 2011. The periplasmic chaperone Skp is required for successful ***Salmonella*** Typhimurium infection in a murine typhoid model. ***Microbiology*** 157: 848 – 858.
14. Man, A. L., E. Bertelli, S. Rentini, M. Regoli, G. Briars, M. Marini, A. J. Watson, and C. Nicoletti. 2015. Age-associated modifications of intestinal permeability and innate immunity in human small intestine. ***Clin. Sci.*** 129: 515 – 527.
15. Di Bella, A., M. Regoli, C. Nicoletti, L. Ermini, L. Fonzi, and E. Bertelli. 2009. An appraisal of intermediate filament expression in adult and developing pancreas: vimentin is expressed in ***α*** cells of rat and mouse embryos. ***J. Histochem. Cytochem.*** 57: 577 – 586.
16. Regoli, M., C. Borghesi, E. Bertelli, and C. Nicoletti. 1994. A morphological study of the lymphocyte traffic in Peyer's patches after an in vivo antigenic stimulation. ***Anat. Rec.*** 239: 47 – 54.
17. Beal, R. K., C. Powers, P. Wigley, P. A. Barrow, and A. L. Smith. 2004. Temporal dynamics of the cellular, humoral and cytokine responses in chickens during primary and secondary infection with ***Salmonella enterica*** serovar Typhimurium. ***Avian Pathol.*** 33: 25 – 33.
18. Nicoletti, C., and C. Borghesi-Nicoletti. 1992. Detection of autologous anti-idiotypic antibody-forming cells by a modified enzyme-linked immunospot (ELISPOT). ***Res. Immunol.*** 143: 919 – 925.
19. Schulz, O., E. Jaensson, E. K. Persson, X. Liu, T. Worbs, W. W. Agace, and O. Pabst. 2009. Intestinal $CD103^{+}$ but not CX_3CR1^{+}, antigen sampling cells migrate in lymph and serve classical dendritic cell functions. ***J. Exp. Med.*** 206: 3101 – 3114.
20. Man, A. L., F. Lodi, E. Bertelli, M. Regoli, C. Pin, F. Mulholland, A. R. Satoskar, M. J. Taussig, and C. Nicoletti. 2008. Macrophage migration inhibitory factor plays a role in the regulation of microfold (M) cell-mediated transport in the gut. ***J. Immunol.*** 181: 5673 – 5680.
21. Bain, C. C., C. L. Scott, H. Uronen-Hansson, S. Gudjonsson, O. Jansson, O. Grip, M. Guilliams, B. Malissen, W. W. Agace, and A. M. Mowat. 2013. Resident and pro-inflammatory macrophages in the colon represent alternative context-dependent fates of the same $Ly6C^{hi}$ monocyte precursors. ***Mucosal Immunol.*** 6: 498 – 510.
22. Martinoli, C., A. Chiavelli, and M. Rescigno. 2007. Entry route of ***Salmonella typhimurium*** directs the type of induced immune response. ***Immunity*** 27: 975 – 984.
23. Iwasaki, A. 2007. Mucosal dendritic cells. ***Annu. Rev. Immunol.*** 25: 381 – 418.
24. Medina-Contreras, O., D. Geem, O. Laur, I. R. Williams, S. A. Lira, A. Nusrat, C. A. Parkos, and T. L. Denning. 2011. CX_3CR1 regulates intestinal macrophage homeostasis, bacterial translocation, and colitogenic Th17 responses in mice. ***J. Clin. Invest.*** 121: 4787 – 4795.
25. Martinez-Argudo, I., and M. A. Jepson. 2008. ***Salmonella*** translocates across an in vitro M cell model independently of SPI-1 and SPI-2. ***Microbiology*** 154: 3887 – 3894.
26. Jepson, M. A., and M. A. Clark. 2001. The role of M cells in ***Salmonella*** infection. ***Microbes Infect.*** 3: 1183 – 1190.
27. Coombes, J. L., B. A. Charsar, S. J. Han, J. Halkias, S. W. Chan, A. A. Koshy, B. Striepen, and E. A. Robey. 2013. Motile invaded neutrophils in the small intestine of ***Toxoplasma gondii***-infected mice reveal a potential mechanism for parasite spread. ***Proc. Natl. Acad. Sci. USA*** 110: E1913 – E1922.